at which point the damping function has reached 0.85 in value, even if the inner model predicts $\ell/\delta > 0.089$. If at $y^+ = 50$ the inner model [Eq. (5)] predicts $\ell/\delta \leq 0.089$, then all aspects of the model are exactly as given by Model 2A. If, however, at $y^+ = 50$, Eq (5) predicts $\ell/\delta < 0.089$, then the mixing length in the outer region becomes constant at

$$\ell = 0.41(1\text{-}e^{-50/26})50\mu_w/\rho_w(\tau_w/\rho_w)^{1/2} \quad (7)$$

which is the value of ℓ at $y^+ = 50$ according to Eq. (5). The choice of $y^+ = 50$ in Eq. (7) was arbitrary, but the motivating concept of preserving the fully turbulent (logarithmic) portion of the velocity profile is supported by available low Reynolds number velocity profile measurements.[14-17]

The results of using Model 2B for incompressible turbulent flow are shown in Fig. 1. Model 2B predicts skin friction coefficients which are slightly higher (6% for $Re_\theta = 450$) for $Re_\theta < 850$ than those predicted by Model 2A; however, from the available data a conclusive case cannot be made for the accuracy of either model over the other. For compressible flow, however, the predictions of Model 2B are dramatically superior to Model 2A at low Reynolds numbers. A representative comparison with the skin-friction coefficient measurements of coles[14] for nominal Mach numbers of 4.5 and 2.6 and Korkegi[17] for a Mach number of 5.8 is shown in Fig. 2. The point of divergence between the two models is seen to translate to larger values of Re_θ as the Mach number increases.

Velocity profiles are predicted quite well at low Reynolds numbers by Type 2 models although space limitations do not permit examples to be presented here. The proposed low Reynolds number modification makes no discernable difference to the predicted velocity profiles for incompressible flows but Model 2B noticeably outperforms model 2A for low Reynolds number compressible flows.

References

[1] Cebeci, T., "Calculation of Compressible Turbulent Boundary Layers with Heat and Mass Transfer," *AIAA Journal,* Vol. 9, June 1971, pp. 1091-1097.

[2] Herring, H.J. and Mellor, G.L., "A Method of Calculationg Compressible Turbulent Boundary Lyers," NASA CR-1144, 1968.

[3] Patankar, S.V. and Spalding, D.B., *Heat and Mass Transfer in Boundary Layers,* 2nd ed., International Textbook Co., London, 1970, pp. 20-21.

[4] Pletcher, R.H., "On a finite Difference Solution for the Constant Property Turbulent Boundary Layer," AIAA Journal, Vol. 7, Feb. 1969, pp. 305-311.

[5] Pletcher, R.H. "On a Calculation Method for Compressible Turbulent Boundary Layer Flows with Heat Transfer," AIAA Paper 71-165, New York, N.Y. 1971.

[6] McDonald,H., "Mixing Length and Kinematic Eddy Vicosity in a Low Reynolds Number Boundary Layer," United Aircraft Research Lab. Rept. J2 14453-1, Sept. 1970, East Hartford, Conn.

[7] Cebeci, T., "Kinematic Eddy Viscosity at Low Reynolds Numbers," *AIAA Journal,* Vol. 11, Jan. 1973, pp. 102-104.

[8] Simpson, R.L., "Characteristics of Turbulent Boundary Layers at Low Reynolds Numbers with and Without Transpiration," *Journal of Fluid Mechanics,* Vol. 42, July 1970, pp.769-802.

[9] Huffman, D.G. and Bradshaw, P., "A Note on von Karman's constant in Low Reynolds Number Turbulent Flows," *Journal of Fluid Mechanics,* Vol. 53, May 1972, pp. 45-60.

[10] Pletcher, R.H., "Prediction of Transpired Turbulent Boundary Layers," *Journal of Heat Transfer,* Vol. 96, Feb. 1974, pp.89-94.

[11] Simpson, R.L., "The Turbulent Boundary Layer on a Porous Plate: An Experimental Study of the Fluid Dynamic with Injection and Suction," Ph.D. dissertation, Dept. of Mechanical Eng., Stanford Univ. Stanford, Calif., Dec. 1967.

[12] Squire, L.C., "The Constant Property Turbulent Boundary Layer with Injection ; a Reanalysis of Some Experimental Results," *International Journal of Heat and Mass Transfer,* Vol. 13, May 1970, pp. 939-942.

[13] Baker, R.J. and Launder, B.E., "The Turbulent Boundary Layer with Foreign Gas Injection: I. Measurements in Zero Pressure Gradient," *International Journal of Heat and Mass Transfer,* Vol. 17, Feb. 1974, pp.275-291.

[14] Coles, D.E., "Measurements in the boundary Layer on a Smooth flat Plate in Supersonic flow, III," Jet Prop. Lab.,Pasadena, Calif. Rept. 20-70, 1953.

[15] Anderson, P.S., Kays W.M., and Moffat, R.J., "The Turbulent Boundary Lyer on a Porous Plate: An Experimental Study of the Fluid Mechanics for Adverse Free-Stream Pressure Gradients," Department of Mechanical Engineering, Stanford Univ., Stanford, Calif., Rept. HMT-15 May 1972.

[16] Coles, D.E. and Hirst, E.H., eds., *Proceedings, Computation of Turbulent Boundary Layers,* Vol. II, Stanford Univ. Stanford, Calif., 1969.

[17] Korkegi, R.H., "Transition Studies and Skin-Friction Measurements on an Insulated Flat Plate at a Mach Number of 5.8," *Journal of the Aeronautical Sciences,* Vol. 25, Feb. 1956, pp.97-192

Concentrated Vortex on the Nose of an Inclined Body of Revolution

T.Hsieh*
Arnold Research Organization, Inc., Arnold Air Force Station, Tenn.

and

K.C. Wang†
Martin Marietta Laboratories, Baltimore, Md.

Introduction

WERLE[1] published in 1962 a series of experimental, incompressible surface-flow patterns over both pointed and blunted bodies of revolution at various incidences. In one of these pictures, there appears a vortex pattern on the leeside front nose (Fig. 1a). The accompanying sketch (Fig. 1b) made by Werle shows the limiting streamlines and a clockwise vortex.

Werle did not discuss how, and under what conditions, such a vortex would occur. Since then, little additional understanding of this problem has been developed. Furthermore, it appears that no similar vortex has been reported in later experiments of surface-flow visualization on similar configurations, for example, those by Stetson[2] and by Zakkay et al.[3], among many others. The latter fact has led to suspicion as to whether the vortex reported by Werle is real, or is caused merely by unsteadiness of the test condition.

Recently one of us (Hsieh)[4] carried out experiments of surface-flow visualization for a hemisphere-cylinder by injecting oil through the model surface at Mach numbers 0.6-1.4 and at incidence angles of 0-19°. A vortex pattern similar to that reported by Werle was observed at higher Mach numbers (1-1.4) and higher incidences (15-19°). Samples are shown in Figs. 2a and 2b.

Proposed Mechanism

In this Note, we propose a possible mechanism for the formation of such a nose vortex within the context of the open-and-closed separation idea. Several years ago, one of us (Wang)[5] pointed out that the separation pattern over an elongated body of revolution (for example, an ellipsoid of revolution) differs from prior conceptions (Fig. 3a). It actually changes from a closed separation at low incidence (Fig.

Received Jan. 15, 1976. This work was supported by the Air Force Flight Dyanmics Laboratory, Wright-Paterson Air Force Base and by the Air Force Office of Scientific Research under contract F44620-70-0085.

Index category: Boundary Layers and Convective Heat Transfer – Laminar.

*Research Engineer. Member AIAA.

†Senior Scientist. Member AIAA.

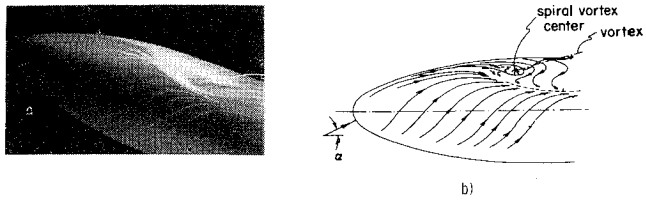

Fig. 1 a) Werle's experiment; b) sketch, $M=0$, $\alpha=20°$.

Fig. 2 Hsieh's experiments; a($M=1,\alpha=15°$,b) $M=1.2$, $\alpha=19°$.

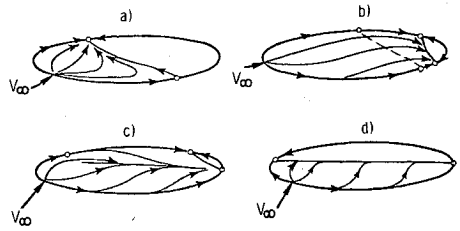

Fig.3 Separation patterns; a) conventional, b) closed at low incidence, c) open at high incidence, d) closed at very high incidence.

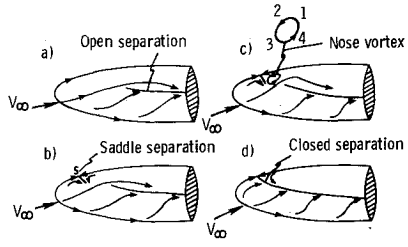

Fig.4 Vortex formation on a blunt body.

3b), to an open separation at moderate to high incidence (Fig. 3c). At still higher incidence, or for a very blunt body, a closed separation prevails again (Fig. 3d). By closed or open, we mean that the separation line does or does not form a closed curve on the body surface. The idea of an open separation has been supported by experiments[2-4] and by calculations.[6,7]

In the case of the vortex shown by Werle, we start by considering the flow involving an open separation at moderate incidence as depicted in Fig. 4a. Then, an increase of incidence leads to the initiation of a local separation which originates at the front leeside saddle separation point, S,(Fig. 4b) and extends laterally away from the plane of symmetry; meanwhile, the open separation line extends forward. As this process develops to a certain stage, a vortex pattern can be constructed as shown in Fig. 4c. The reversed flow caused by the local separation near point S follows the upper path ($1\rightarrow2\rightarrow3$), whereas the open separation permits the flow to enter the leeside region along the lower path ($3\rightarrow4\rightarrow1$); thus, a closed vortex path is formed. Note that the direction of rotation is opposite to that suggested by Werle (Fig. 1b). If the incidence is increased further, the separation would become completely closed, and the isolated vortex would disappear. Based on this reasoning, the vortex occurs only during the transition from an open separation to a completely closed separation.

In the case of the vortex in Hsieh's experiment, the flow at a fixed Mach number may start at zero incidence, with a

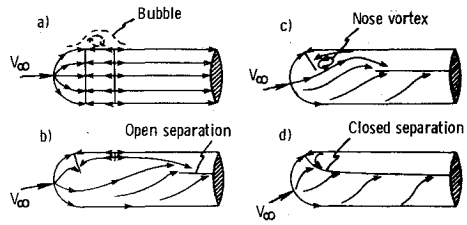

Fig.5 Vortex formation on a hemisphere-cylinder.

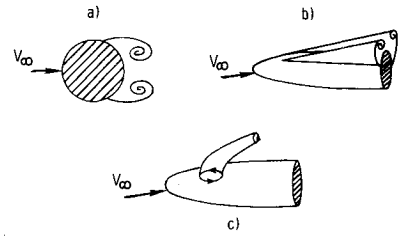

Fig.6 Different vortices; a) transverse vortex, b) streamwise vortex, c) present.

separation bubble near the junction of the hemisphere and the cylinder (Fig. 5a). At low incidence, the separation bubble on the windward surface gradually disappears, whereas that on the leeward surface moves slightly forward; meanwhile, an open separation line emerges over the aft-body (Fig. 5b). As the incidence further increases, the open separation line extends farther forward. Under this condition, a vortex pattern again can be constructed (Fig. 5c). It is expected, but not yet tested experimentally, that continuing increase of incidence will lead finally to a completely closed separation (Fig. 5d). Thus, in this hemisphere-cylinder case, the flow starts somewhat differently with a separation bubble, but the process of the vortex formation goes very much the same way as in the preceding case.

The resulting vortex presents interesting contrasts with other familiar ones. Although our discussion on the possible vortex-formation has been limited to surface-flow behavior, it seems that some comparisons can be drawn reasonably. For the transverse vortex in a two-dimensional flow, the vortex axis is always perpendicular to the freestream and parallel to the body generator. A typical example is the vortices behind a cylinder (Fig. 6a, not necessarily circular). For the streamwise vortex in a three-dimensional flow, the vortex axis is oriented (or approximately oriented) along the freestream. Figure 6b illustrates an example for the flow over an inclined body of revolution. For the present vortex (Fig. 6c), the vortex axis is, at first, normal to the body surface and is convected downstream above the body. Both the streamwise vortex and the present vortex occur only in three-dimensional flow; the streamwise vortex acquires its vorticity from the transverse component of flow, prevails under more general conditions, and extends all along the body (at least for the body in Fig. 6b). The present vortex results from the combined effects of both longitudinal and transverse components (or meridional and circumferential components) of a boundary-layer flow; it occurs only under special circumstances (a narrow range of incidence), and rises from the surface out into the flow somewhat like a tornado in the atmosphere. It is, of course, understood that there is a pair of such nose vortices, symmetrically situated on two sides of the plane of symmetry, though we have referred to and sketched only one vortex in the preceding discussion.

In terms of practical application, we note that one often attempts to measure the flow conditions by placing instrumentation on the leeside of the body. In doing this, it is clear that the measurements must be not influenced by the presence of such nose vortices.

Conclusions

The nose vortex observed by Werle and Hsieh is explained on the basis of separation patterns previously discussed by Wang. It is counterclockwise rather than clockwise, as implied in Werle's original sketch. It occurs only during the transition from an open separation to a completely closed separation over an inclined body. Because it occurs only under this limited circumstance, such vortex formation easily can go unnoticed, unless one searches for it. Calculation of such a nose vortex appears to require a complete Navier-Stokes approach, and is a task for the future. Note added during proof: Werle has just sent us two surface-flow pictures for a nearly-flat blunt-nosed cylinder at $\alpha = 10°$ and 15° which also indicates a vortex pattern similar to those in Figs. 2a and b.

References

[1] Werle, H., "Separation on Axisymmetrical Bodies at Low Speed," *La Recherche Aeronautique,* No. 90, Sept.-Oct. 1962 pp. 3-14.

[2] Stetson, K.F., "Boundary-Layer Separation on Slender Cones at Angle of Attack," *AIAA Journal,* Vol. 10, May 1972,pp. 642-648.

[3] Zakkay, V., Miyazawa, M., and Wang, C.R., "Lee Surface Flow Phenomena Over Space Shuttle at Large Angles of Attack at $M_\infty = 6$," CR-13250l, 1974, NASA; also AIAA paper 75-148, Jan. 1975.

[4] Hsieh, T., "An Investigation of Separated Flow about a Hemisphere-Cylinder at Zero to 19 deg. Incidences in the Mach Number Range form 0.6 to 1.5," to be published as AECD-TR.

[5] Wang, K.C., "Separation Patterns of Boundary Layer over an inclined Body of Revolution," *AIAA Journal.* Vol. 10, Aug. 1972, pp. 1044-1050.

[6] Wang, K.C., "Boundary Layer over a Blunt Body at High Incidence with an Open-Type of Separation," Proceedings of the Royal Society of London, Series A., Vol., 340, 1974, pp. 33-55.

[7] Geissler, W., "Three-Dimensional Laminar Boundary Layer over a Body of Revolution at Incidence and with Separation," *AIAA Journal,* Vol. 12, Dec. 1974, pp. 1743-1745.

Approximate Statistics of Random Vector Magnitudes

Hamilton Hagar Jr.*
Jet Propulsion Laboratory, Pasadena, Calif.

Introduction

IT often is desirable to know, at least approximately, the mean and 99% value of the magnitude of a random vector with independent components. A related case, for example, is the computation of the corrective velocity 99% statistics in interplanetary spacecraft maneuver analyses. In general, let the random vector be denoted as

$$\bar{v} = \begin{bmatrix} x \\ y \\ z \end{bmatrix} \tag{1}$$

with magnitude $v \equiv |\bar{v}| = (x^2+y^2+z^2)^{1/2}$. If x, y, z are distributed normally, if $E(x) = E(y) = E(z) = 0$, and if $E(x^2) = E(y^2) = E(z^2) = \sigma^2$, then v is distributed Maxwellian with mean $(8/\pi\sigma)^{1/2}$ and variance $(3-8/\pi)\sigma^2$. If the vector is a two-vector, say, $z \equiv 0$ in v, then the distribution of v is Rayleigh, with mean $(\pi/2)^{1/2}\sigma$ and variance $(2-\pi/2)\sigma^2$. A half-normal distribution results for $v = |x|$, with mean $(2/\pi)^{1/2}\sigma$ and variance $(1-2/\pi)\sigma^2$. These are special cases of χ distributions with degrees of freedom of 3, 2, 1, respectively (see, e.g., Refs. 1 and 2). The 99% values can be obtained directly from tables (e.g., Ref. 3) and for these cases are $v_{99} = 3.368\sigma$, $v_{99} = 3.035\sigma$, and $v_{99} = 2.576\sigma$, respectively.

The preceding, however, are very special cases, not applicable, in general, where the variances of x, y, and z are unequal. Although the case where $E(x^2) = E(y^2) = \sigma^2$, $E(z^2) = s^2$ is known,[4] and the general case for $E(x^2) = \sigma^2$, $E(y^2) = r^2$, and $E(z^2) = s^2$ has been solved,[5,6] generally these are computationally demanding. The next section presents simple, rough approximations for the mean and 99% values for random vectors of up to three independent elements.

Note that, when the elements of $\bar{v}$ are correlated, the problem may be reduced to the independent case by an appropriate transformation, $\bar{w} \equiv R\bar{v}$, so that

$$E(\bar{w}\bar{w}^T) = RE(\bar{v}\bar{v}^T)R^T = RVR^T = W \tag{2}$$

W is a diagonal matrix whose elements are the eigenvalues (all real) of the covariance matrix V; the columns of R are the corresponding eigenvectors. Because V is symmetric, $R^T = R^{-1}$; hence,

$$w = (\bar{w}^T\bar{w})^{1/2} = (\bar{v}^T R^T R\bar{v})^{1/2} = (\bar{v}^T\bar{v})^{1/2} = v \tag{3}$$

Development

A workable approach to approximating the mean and 99% values where x, y, and z have unequal variances can be obtained as functions of the means and 99% values for the respective individual cases with equal variances. Three forms for the approximation of both are

$$\alpha = \{c_1\sigma^2 + (c_2-c_1)(r^2+s^2)[(c_3-c_2)-(c_2-c_1)]rs\}^{1/2} \tag{4}$$

$$\beta = [c_1\sigma^2 + (c_2-c_1)r^2 + (c_3-c_2)s^2]^{1/2} \tag{5}$$

$$\gamma = (c_1)^{1/2}\sigma + [(c_2)^{1/2} - (c_1)^{1/2}]r + [(c_3)^{1/2} - (c_2)^{1/2}]s \tag{6}$$

where α, β, and γ represent either the mean or 99% value, $\sigma^2 = E(x^2)$, $r^2 = E(y^2)$, $s^2 = E(z^2)$, and c_1, c_2, and c_3 are coefficients associated with the one-, two-, and three- element vectors. These coefficients are presented in Table 1. They are the squares of the mean values and 99% values given in the Introduction. Thus, for the cases where 1) $\sigma = r = s$, 2) $\sigma = r$,

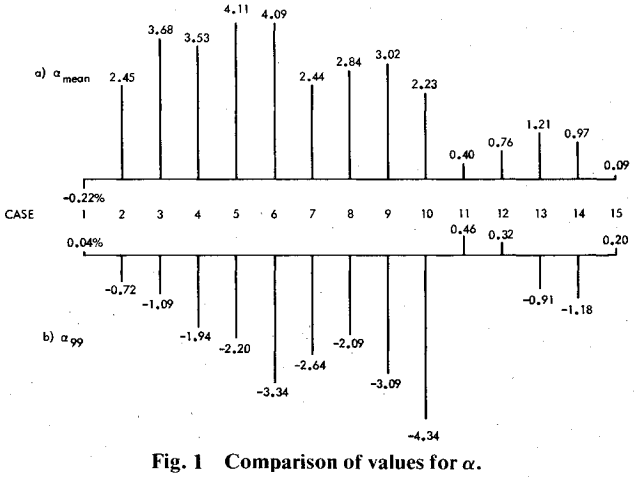

Fig. 1 Comparison of values for α.

Received Sept. 29, 1975; revision received March 5, 1976. This paper presents the results of one phase of research carried out at the Jet Propulsion Laboratory, California Institute of Technology, under Contract NAS7-100, sponsored by NASA.

Index categories: Aerospace Technology Utilization; Navigation, Control, and Guidance Theory; Spacecraft Mission Studies and Economics.

*Member of the Technical Staff. Member AIAA.